

# Assessment of stochastic weather forecast of precipitation near European cities, based on analogs of circulation

Meriem Krouma <sup>1,2</sup>, Pascal Yiou <sup>2</sup>, Céline Déandreis <sup>1</sup>, and Soulivanh Thao <sup>2</sup>

<sup>1</sup>ARIA Technologies, 8 Rue de la Ferme, 92100 Boulogne-Billancourt, France

<sup>2</sup>Laboratoire des Sciences du Climat et de l'Environnement, UMR 8212 CEA-CNRS-UVSQ, IPSL & Université Paris-Saclay, 91191 Gif-sur-Yvette, France

**Correspondence:** Meriem Krouma (meriem.krouma@lsce.ipsl.fr)

## Abstract.

In this study, we aim to assess the skill of a stochastic weather generator (SWG) to forecast precipitation in several cities of Western Europe. The SWG is based on random sampling of analogs of the geopotential height at 500 hPa. The SWG is evaluated for two reanalyses (NCEP and ERA5). We simulate 100-member ensemble forecasts on a daily time increment. We evaluate the performance of SWG with forecast skill scores and we compare it to ECMWF forecasts. Results show significant positive skill score (continuous rank probability skill score and correlation) for lead times of 5 and 10 days for different areas in Europe.

We find that the low predictability of our model is related to specific weather regimes, depending on the European region. Comparing SWG forecasts to ECMWF forecasts, we find that the SWG shows a good performance for 5 days. This performance varies from one region to another. This paper is a proof of concept for a stochastic regional ensemble precipitation forecast. Its parameters (e.g. region for analogs) must be tuned for each region in order to optimize its performance.

## 1 Introduction

Ensemble weather forecasts were designed to overcome the issues of meteorological chaos, from which small uncertainties in initial conditions can lead to a wide range of possible trajectories (Sivillo et al., 1997; Palmer, 2000). Hence, from a sufficiently large ensemble of initial conditions, it is in principle possible to sample the probability distribution of future states of the system.

Forecasts issued by meteorological centers are obtained by computing several simulations with perturbed initial conditions, in order to sample uncertainties. Those experiments are rather costly in terms of computing resources and are generally limited to a few tens of members (Hersbach et al., 2020; Toth and Kalnay, 1997), which can hinder a proper estimate of probability distributions of trajectories. Moreover, obtaining information at local spatial scales can be difficult because the horizontal resolution of the atmospheric models is around 18 km, e.g. for the European Centre for Medium-Range Weather Forecasts (ECMWF) ensemble forecast system.

From a mathematical point of view, computing the probability distribution of the trajectories of a (deterministic) system makes the underlying assumption that the system behaves like a stochastic process, for which statistical properties are defined naturally (Ruelle, 1979; Eckmann and Ruelle, 1985). This has justified the development of stochastic weather generators

25 (SWG), which are stochastic processes that emulate the behavior of key climate variables (Ailliot et al., 2015). The advantages of stochastic models are a relative simplicity of implementation and a low computing cost. The challenge of their development is to verify that the behavior of the simulations are realistic, according to well-defined criteria (van den Dool, 2007; Jolliffe and Stephenson, 2011).

The first stochastic weather generators were devised to simulate rainfall occurrence by Gabriel and Neumann (1962) and  
30 to simulate rainfall amounts by Todorovic and Woolhiser (1975). SWGs were developed and used to estimate the probability distributions of climate variables such as temperature, solar radiation, and precipitation through extensive simulations (Richardson, 1981).

Stochastic weather generators can be useful complements to atmospheric circulation models, in order to simulate large ensembles of local variables, as they can be calibrated for small spatial scales comparing to numerical models (Ailliot et al.,  
35 2015). This explains their wide applications in impact studies.

A successful simulation with SWG relies on the choice of inputs. One of them consists in the use of the atmospheric circulation as a predictor for other local variables. The (loose) rationale for this choice is that the circulation is modeled by prognostic equations (Peixoto and Oort, 1992), that drive the other physical variables. Therefore the primitive equations of the atmosphere (Peixoto and Oort, 1992, Chap. 3) suggest that reproducing temporal variability on daily time scales requires considering circula-  
40 tion variables. The influence of large-scale circulation on local climate variables has been proven in previous studies such as the influence of atmospheric circulation on Mediterranean Basin (Mastrantonas et al., 2021) and Greece precipitation (Xoplaki et al., 2000; Türkeş et al., 2002). Similar influences have been found on precipitation and temperature over the North Atlantic region (Jézéquel et al., 2018b).

Analogs of circulation were initially designed to provide "model-free" forecasts, by assuming that similar situations in atmospheric circulation may lead to similar local weather conditions (Lorenz, 1969). The potential to simulate large ensembles of forecasts temperature with circulation analogs was explored by Yiou and Déandréis (2019), by considering random resamplings of  $K$  best analogs (rather than only considering the best analog). This has led to the development of a SWG in "predictive" mode, which uses updates of reanalysis datasets (Kistler et al., 2001) as input.

Alternative systems of analogs to forecast precipitation have been proposed by Atencia and Zawadzki (2014). Those systems  
50 are based on analogs of precipitation itself. Such systems are very efficient for nowcasting, i.e. forecasting precipitation within the next few hours. Considering the atmospheric circulation analogs allows to focus on longer time scales.

Yiou and Déandréis (2019) evaluated ensemble forecasts of the analog SWG for temperature and the NAO index with classical probability scores against climatology and persistence. Reasonable scores were obtained up to 20 days. Through this study, we aim to assess the skill of this SWG to forecast precipitation in different areas of Europe and for different lead times.  
55 The previous study on this forecast tool was a proof of concept for temperature. In this study we will adapt the parameters of the analog SWG to optimize the simulation of European precipitations. We then analyse the performance of this SWG for lead times of 5 to 20 days, with the forecast skill scores used by Yiou and Déandréis (2019).

We will evaluate the seasonal dependence of the forecast skills of precipitation and the conditional dependence to weather regimes. Finally, comparisons with medium range precipitation forecasts from the ECMWF will be performed.

60 The paper is divided as follows: Section 2 is dedicated to describe the data used for the experiments. Section 3 explains the methodology (analogs and stochastic weather generator) and experimental set up. Section 4 details results of simulations and the evaluation of the ensemble forecast. Section 5 contains the main conclusions of the analyses.

## 2 Data

Daily precipitation data were obtained from the European Climate Assessment and Data (ECAD) project (Klein Tank et al., 65 2002) for four locations in western Europe (Berlin, Madrid, Orly, Toulouse), which are subject to contrasted meteorological influences (Figure 1). ECAD provides station data, that are available at a daily time step from 1948 to 2019. The choice of those stations was based on the availability of large and common period of observations with a low rate of missing data (less than 10%). For verification issues, we used also the E-Obs data (Haylock et al., 2008), which are a daily gridded data available from 1979 to present with a horizontal resolution of  $0.25^\circ \times 0.25^\circ$ . E-Obs data are spatial interpolations of ECAD data.

70 We recovered the geopotential height at 500 hPa (Z500) and sea level pressure (SLP) fields from the reanalysis of the National Centers for Environmental Prediction (NCEP: Kistler et al. (2001)) with a spatial resolution of  $2.5^\circ \times 2.5^\circ$  from 1 January 1948 to 31 December 2019.

We also used the atmospheric reanalysis (version 5) of the European Centre for Medium-Range Weather Forecasts (ECMWF) (ERA5; Hersbach et al. (2020)). ERA5 data are available from 1950 to present with a horizontal resolution of  $0.25^\circ \times 0.25^\circ$ . 75 There are fundamental differences between the two reanalyses, in the atmospheric models, assimilated data, and assimilation schemes.

We considered the daily averages of Z500 from NCEP and ERA5, over the region covering  $30^\circ\text{W} - 20^\circ\text{E}$  and  $40^\circ - 60^\circ\text{N}$  to compute circulation analogs. Daily averages of SLP were used over the region covering  $80^\circ\text{W} - 20^\circ\text{E}$  and  $30^\circ - 70^\circ\text{N}$  to define weather regimes.

80 In order to assess the predictive skill of our precipitation forecast model, a comparison with another forecast was made. There are many available datasets that can be used for deriving this information. We considered the ECMWF ensemble forecast dataset system 5 (Vitart et al., 2017). It is a daily gridded dataset interpolated over Europe to provide information covering the all the domain. Data are available through the Copernicus Climate Data Store including forecasts created in real-time (since 2017) and hindcast forecasts from 1993 to 2019 (Vitart et al., 2017). The data are provided at an hourly time step with a 85 horizontal resolution of  $0.25^\circ \times 0.25^\circ$ . We considered the grid points that include Berlin, Orly, Toulouse and Madrid, which were identified in the ECAD database.

## 3 Methodology

### 3.1 Analogs

The first step is to build a database of analogs of the atmospheric circulation. We outline the procedure of Yiou and Déandréis 90 (2019), summarized in Figure 1a. For a given day  $t$ , we determine the similarity of Z500 for all days  $t'$  that are within 30

calendar days of  $t$  but in a different year from  $t$ . The similarity is quantified by a Euclidean distance (or root mean square) between the daily Z500 maps. Other types of distances are possible (Blanchet et al., 2018), but the expected impact on the results is often marginal (Toth, 1991). We believe that the simplicity of the a Euclidean distance makes it more robust to changes in horizontal resolution (e.g. from NCEP to ERA5), compared to more sophisticated distances that include local spatial gradients, which would require adjustments and additional tuning. This choice can be left open for future fine tuning, depending on the region.

For each day  $t$ , we consider the  $K = 20$  best analogs, i.e. for which the distances are the smallest. The choice of  $K = 20$  analogs was based on numerical experiments: we considered 20 analogs to ensure that we have enough analog dates for the simulations, and it appears that the Euclidean distance of analogs grows rather slowly after  $K = 20$ . Our choice was also comforted by a theoretical study by (Platzer et al., 2021) who showed that, for complex systems, the use of a large number of analogs ( $K > 30$  analogs) does not change much the prediction properties with analogs. We compute the spatial rank correlation between the Z500 best analogs and the Z500 at time  $t$  for a posteriori verification purposes.

As a refinement over the study of Yiou and Déandréis (2019), a time embedding of 4 days was used for the search of analogs dates. This means that the field  $X(t)$  for which we compute analogs is  $X(t) = (Z500(t), Z500(t+1), \dots, Z500(t+3))$ . This ensures that temporal derivatives of the atmospheric field are preserved (Yiou et al., 2013). Hence the distance that is optimized to find analogs of the  $Z500(x, t)$  field is:

$$D(t, t') = \left[ \sum_x \left( \sum_{i=0}^3 |Z500(x, t+i) - Z500(x, t'+i)| \right)^2 \right]^{\frac{1}{2}}, \quad (1)$$

where  $x$  is a spatial index.

We consider different geographic domains as showed in Figure 1 for the computation of analogs and weather regimes. The computation of circulation analogs was performed with the "blackswan" Web Processing Service (WPS, Hempelmann et al. (2018)). The "blackswan" WPS is an online tool that helps computing circulation analogs on various datasets (reanalyses, climate model simulations) with a user friendly interface.

### 3.2 Configuration of stochastic weather generator

We use a stochastic weather generator (SWG) based on a random sampling of the circulation analogs. The operation of the SWG and its design are detailed by Yiou and Déandréis (2019). The aim is to generate random trajectories from the previously computed analogs. Therefore, to generate a trajectory, we proceed as follows. For a given day  $t_0$  in year  $y_0$ , we generate a set of  $N = 100$  simulations until a time  $t_0 + T$ , with a lead time  $T \in \{5, 10, 20\}$  days. We start at day  $t_0$  and randomly select an analog (out of  $K = 20$ ) of day  $t_0 + 1$ . The random selection of analogs of day  $t_0 + 1$  is performed with weights that are proportional to the calendar difference between  $t_0$  and analog dates, to ensure that time goes forward. We also exclude analog dates with years that are equal to  $y_0$ . This rule is important for the next iterations. We then replace  $t_0$  by the selected analog of  $t_0 + 1$  and repeat the operation  $T$  times. Excluding analog selection in year  $y_0$  ensures that we do not use information from the  $T$  days that follow  $t_0$ . Hence we obtain a hindcast trajectory between  $t_0$  and  $t_0 + T$ .

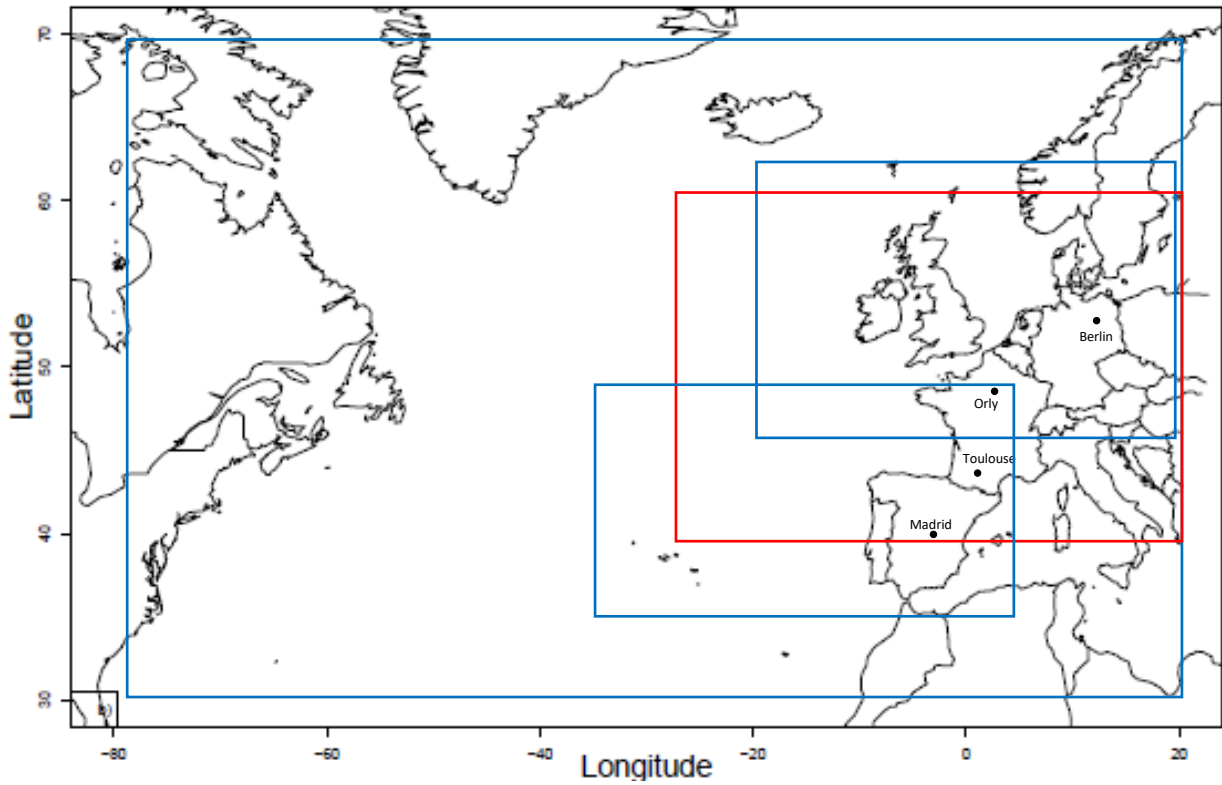
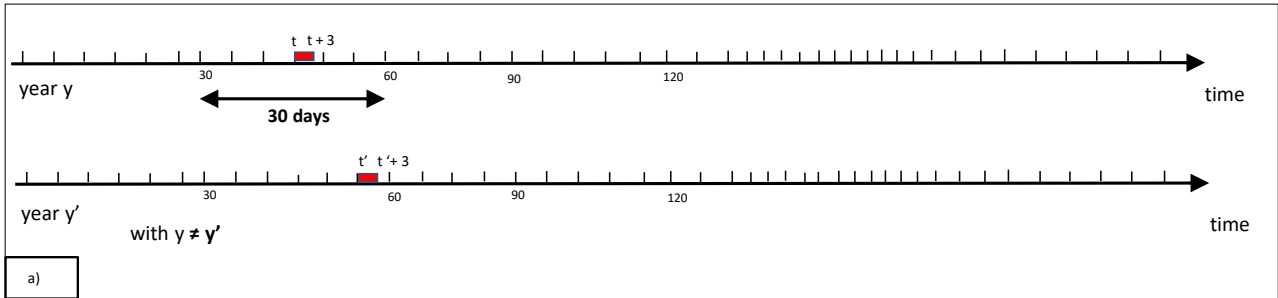


**Figure 1.** Parameters of the analog computation. (a) For each day  $t$  in year  $y$ , we chose an analog day  $t'$  with a similar sequence of 4 consecutive day Z500 patterns.  $t'$  is selected within 30 calendar days of  $t$ , and in a year  $y' \neq y$ . (b) Domains of computation of analogs, we computed analogs over different domains, each one includes a part of the Atlantic and focus in a part of Western Europe, in order to test the sensitivity of our model to different geographic areas, the optimising area was [30°W-20°E; 40°-60°N], indicated by the red rectangle.

This operation of trajectory simulation from  $t_0$  to  $t_0 + T$  is repeated  $N = 100$  times. The daily precipitation of each trajectory is time-averaged between  $t_0$  and  $t_0 + T$ . Hence, we obtain an ensemble of  $N = 100$  forecasts of the average precipitation for day  $t_0$  and lead time  $T$ .

Then  $t_0$  is shifted by  $\Delta t \geq 1$  days, and the ensemble simulation procedure is repeated. This provides a set of ensemble forecasts with analogs.

We made a hindcast exercise where the forecasts of precipitations based on atmospheric circulation (Z500) are started every  $\Delta t \approx T/2$  day between January 1, 1948 and December 31, 2019. This yields a stochastic ensemble hindcast of precipitation and atmospheric circulation (Z500). In this paper, we therefore analyze the properties of an ensemble forecast of mean precipitation between  $t_0$  and  $t_0 + T$ . To evaluate our forecasts, the predictions made with the SWG are compared to the persistence and climatological forecasts. The persistence forecast consists of using the average value between  $t_0 - T$  and  $t_0$  for a given year. The climatological forecast takes the climatological mean between  $t_0$  and  $t_0 + T$ . The two "reference" forecasts are randomized by adding a small Gaussian noise, whose standard deviation is estimated by bootstrapping over  $T$  long intervals. We thus generate sets of persistence forecasts and climatological forecasts that are consistent with the observations (Yiou and Déandréis, 2019).

The simulations of this stochastic model will be called "SGW forecasts", as opposed to ECMWF forecasts.

### 3.3 Forecast Verification

Forecast verification is the process of determining the statistical quality of forecasts. A wide variety of ensemble forecast verification procedures exists. They involve measures of the relationship between a set of forecasts and corresponding observations. To assess the quality of precipitation forecasts, we compute indicators such as the Correlation and Continuous Rank Probability Skill Score (CRPSS) for each lead time  $T$ , for different seasons and months.

The temporal rank correlation is calculated between the precipitation observations and the median of 100 simulations. This simple diagnostic is often used to assess forecast skills of indices (Scaife et al., 2014).

The continuous ranked probability score (CRPS) represents the most used score for probability forecast verifications (Ferro, 2007). It is sensitive to the distance between forecast and observation probability distributions.

If the ensemble forecast yields a probability distribution  $P(x)$ , the CRPS measures how is the probability distribution of  $x$  (Hersbach, 2000).

The CRPS is computed as:

$$CRPS(P, x_a) = \int_{-\infty}^{+\infty} (P_t(x) - P_{a,t}(x))^2 dx, \quad (2)$$

where  $P_a$  represents the Heaviside function of the occurrence of  $x$ . The decomposition and properties of the CRPS have been investigated by (Ferro, 2007; Hersbach, 2000; Zamo and Naveau, 2018). A perfect forecast would have a CRPS equal to 0, but the CRPS value obviously depends on the units of the variable to forecast. It is hence difficult to compare CRPS values

for temperature and precipitation, within the same ensemble forecast. This issue is also acute for non Gaussian variables with heavy tails (Zamo and Naveau, 2018), so that the interpretation of a given CRPS value might not always be informative.

155 One way of circumventing this difficulty is to compare CRPS values to reference forecasts, such as persistence or climatology. The continuous rank probability skill score (CRPSS) is a normalization of Eq. (2) with respect to such a reference.

The CRPSS is hence computed by:

$$CRPSS = 1 - \frac{\overline{CRPS}}{\overline{CRPS}_{ref}} \quad (3)$$

160 where the  $CRPS_{ref}$  is the CRPS of reference forecast (climatology or persistence). The CRPSS is interpreted as a percentage of improvement over a reference forecast.

The values of the CRPSS varies between  $-\infty$  and 1. The forecast is considered to be an improvement over the reference when the CRPSS value is close to 1 (i.e. when the CRPS is 0). Values of CRPSS equal to 0 indicates no improvement over the reference. Values inferior to 0 mean that the forecast is worse than the reference.

We use the CRPSS values to determine the maximum lead time  $T$  for which the SWG forecast is better than references.  
165 Then the SWG assessments will use the CRPS and directly compare the probability distributions of precipitation ensemble forecasts.

### 3.4 Dependence of forecast on weather regimes

We investigate the role of North Atlantic weather patterns on the forecast quality by attributing CRPS values of the SWG precipitation simulations to weather regimes. Weather regimes are defined as large-scale quasi stationary atmospheric states.  
170 They are characterised by their recurrence, persistence and stationarity (Michelangeli et al., 1995). They help describing the features of the atmospheric circulation. Surface variables like temperature and precipitation are largely correlated with weather regimes (van der Wiel et al., 2019).

The North Atlantic weather regimes were computed with the procedure of (Yiou et al., 2008), with the NCEP reanalysis. The first 10 principal components of SLP (large region in Figure 1b) are classified with a k-means algorithm onto four classes, over  
175 a reference period between 1970 and 2010. The procedure is repeated 100 times with random k-means initialization. Then we classify the resulting  $100 \times 4$  k-means weather regimes, in order to determine the most probable classification. This heuristic procedure increases the robustness of the obtained weather regimes. Figure 2 shows four weather regimes for each season (winter and summer) that are coherent with the literature (Cassou et al., 2011; Ghil et al., 2008; Kimoto, 2001; Michelangeli et al., 1995)

180 The winter weather regimes are the Scandinavian blocking (BLO), Atlantic ridge (AR), negative phase of the North Atlantic oscillation (NAO-) and Zonal flow (ZO). The summer weather regimes are the negative phase of the NAO (NAO-), Atlantic ridge (AR), Scandinavian blocking (BLO) and Atlantic low (AL). The regimes are not the same in both seasons, due to the seasonality of the large scale atmospheric circulation.

For each day (in winter and summer) between 1948 and 2019, we classify the SLP by minimizing the root mean square to  
185 four reference (1970–2010) weather regimes.

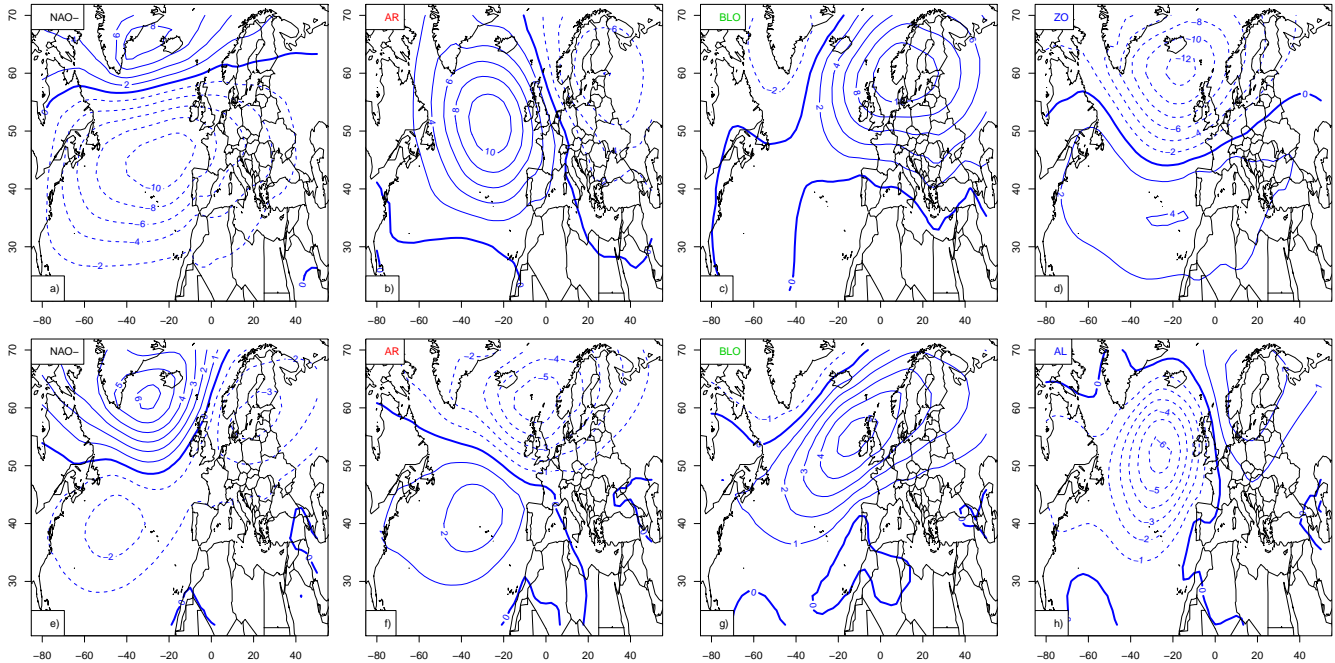


**Figure 2.** Weather regimes over Europe from SLP fields: North Atlantic oscillation (NAO-), the Atlantic ridge (AR), the Scandinavian blocking (BLO), and Atlantic zonal (NAO+). The figure summarises the different states of the atmosphere during summer (a to d) and winter (e to h). It indicates the low and the high pressure over Europe and the direction of flow from the west (Atlantic) to the east. The isolines show seasonal anomalies with respect to a June-July-August and December-January-February means, in hPa with 2 hPa increments.

For each day  $t$  (within a given season), we consider the analogs dates of all  $N = 100$  simulations between  $t$  and  $t + T$  and the corresponding classification into weather regimes. Then we determine the most frequent weather regime of the  $N$  member ensemble forecast between  $t$  and  $t + T$ . We hence obtain times series on the most likely weather pattern that dominates in the ensemble forecast between  $t$  and  $t + T$ .

190 We evaluate the influence of the dominating weather regimes on the SWG forecast quality by plotting the probability distribution of CRPS values *conditional* to each weather regime. This is done separately for "good" forecasts (low CRPS values) and "poor" forecasts (high CRPS values).

We identify two classes of predictability from CRPS values:

- Low predictability is related to high values of CRPS that exceed the 75th quantile,
- 195 – High predictability is linked to low values of CRPS, below the 25th quantile.

Then we associate the dominating weather regimes computed above with classes of high or low predictability. This procedure helps identifying atmospheric patterns that could lead to low or high predictability with the SWG model.



## 4 Results

### 4.1 Parameter optimization

200 To obtain optimal forecasts some parameters have been adjusted. The first parameter is the geographical area. We computed sample trajectories of the SWG for the four domains outlined in Figure 1b. We used different domains in order to find an optimal region which allows verifying the relationship between precipitation and Z500. Each domain includes a part of the Atlantic and a part of western Europe. The widest domain of the coordinates  $80^{\circ}\text{W} - 20^{\circ}\text{E}$  and  $30^{\circ} - 70^{\circ}\text{N}$  did not give good results for precipitation forecasting for the four studied areas in western Europe, while the other two smaller domains (in blue) 205 gave good forecasts for specific locations. However, in order to make a forecast for the whole of Europe, we found that the domain for Z500 analogs that optimizes precipitation correlations is  $30^{\circ}\text{W} - 20^{\circ}\text{E}$  and  $40^{\circ} - 60^{\circ}\text{N}$ . Therefore we kept this domain for the subsequent analyses. We determined that the SWG simulations showed better skills for the geographic domain outlined in red in Figure 1b) as it allows to make forecasts for all the studied areas and we find that the skill scores over this geographic domain remained the highest ones as represented in the following Table 1.

**Table 1.** Correlation between observations and the median of 100 simulations for the winter (DJF) for the different studied domains represented in Figure 1b, with the coordinates  $80^{\circ}\text{W} - 20^{\circ}\text{E}$  ;  $30^{\circ} - 70^{\circ}\text{N}$  for the largest one (blue) and  $30^{\circ}\text{W} - 20^{\circ}\text{E}$  ;  $40^{\circ} - 60^{\circ}\text{N}$  for the red rectangle for a lead time of 5 days.

Location	The domain $80^{\circ}\text{W} - 20^{\circ}\text{E}$ ; $30^{\circ} - 70^{\circ}\text{N}$		The domain $30^{\circ}\text{W} - 20^{\circ}\text{E}$ ; $40^{\circ} - 60^{\circ}\text{N}$	
	Correlation	95% confidence interval	Correlation	95% confidence interval
<b>Berlin</b>	0.32	0.30 – 0.35	0.50	0.48 – 0.56
<b>Madrid</b>	0.35	0.33 – 0.39	0.53	0.51 – 0.55
<b>Orly</b>	0.39	0.37 – 0.41	0.58	0.56 – 0.59
<b>Toulouse</b>	0.34	0.31 – 0.36	0.40	0.39 – 0.44

210 For comparison purposes, SWG simulations are obtained using analogs computed from reanalyses on the NCEP and ERA5 reanalyses. By comparing their skill scores, we found that CRPSS and correlation between observations and simulations are positive in both cases, and showing positive improvement comparing to persistence and climatology forecasts. The CRPSS and correlation for simulations with analogs of NCEP are almost identical to those with ERA5, as showed in Table 2. Therefore, we focus on SWG simulations with analogs from the NCEP reanalysis in the sequel as both NCEP and ERA5 (1950 to 2019) have 215 the same skill as shown in Table 2, and NCEP is easier to handle, as its horizontal resolution is much lower. The computations were made using observations of precipitation from the ECAD and E-Obs. We found the same results because the ECAD and E-Obs are highly correlated (by construction of E-Obs).

We quantify the dependence of the forecast on the time embedding for the analogs by calculating the analogs based on different embedding going from 1 to 4 days. We find that an embedding of 4 days helped to better catch the persistence and 220 improve the skill scores for the forecast compared to 1 day, as shown in Table 3. Therefore we kept the forecast based on a 4-day

**Table 2.** Comparison between the values of the CRPSS of SWG computed using different reanalysis dataset (NCEP, ERA5 (1979 to 2019) and ERA5 extended (1950 to 2019)) for a lead time of  $T = 5$  days for winter (DJF)

Location	CRPSS DJF ERA5	CRPSS DJF ERA5 extended	CRPSS DJF (NCEP)	CRPSS JJA (NCEP)
<b>Berlin</b>	0.47	0.50	0.50	0.21
<b>Madrid</b>	0.50	0.55	0.57	0.25
<b>Orly</b>	0.51	0.53	0.53	0.23
<b>Toulouse</b>	0.39	0.41	0.41	0.24

embedding. This choice was based on the numerical experiments we made for the studied locations. This is also supported by You et al. (2013) where the analog computation with delays was argued to improve the temporal smoothness of simulations. With such an embedding, forecasts for lead times of  $T = 5$  days yield at least two time increments.

**Table 3.** Correlation between observations and the median of 100 simulations for the winter (DJF) based on analogs computed with an embedding of 1 and 4 days for the geographic domain with the coordinates  $30^{\circ}\text{W} - 20^{\circ}\text{E}$  ;  $40^{\circ} - 60^{\circ}\text{N}$  for a lead time of 5 days.

Location	Analog with 1 day time embedding		Analog with 4-day time embedding	
	Correlation	95% confidence interval	Correlation	95% confidence interval
<b>Berlin</b>	0.39	0.37 – 0.43	0.50	0.48 – 0.56
<b>Madrid</b>	0.40	0.38 – 0.42	0.53	0.51 – 0.55
<b>Orly</b>	0.42	0.39 – 0.45	0.58	0.56 – 0.59
<b>Toulouse</b>	0.35	0.34 – 0.37	0.40	0.39 – 0.44

## 4.2 Sample forecast

225 As an example, we illustrate the behavior of the trajectories in Orly for the summer and winter of 2002. Figure 3 shows the observed and simulated values of precipitation for lead times of 5 and 10 days for summer (June–July–August: JJA) and winter (December–January–February: DJF), for Orly precipitation data. We observe significantly positive correlations between observed values and the median of the forecasts, for the four data sets as represented in Table 4 . The correlation is generally smaller in the summer than in the winter. The correlation skill is low for some extremes values of precipitation. For a lead time  
230 of 10 days, SWG simulation still show capacity to predict precipitation especially for winter with a correlation equal to 0.23 (Orly), 0.30 (Berlin), 0.43 (Madrid), 0.31 (Toulouse).

We observe that the 5th and 95th quantiles of simulations include the different values of observations. This heuristically confirms the good skill of SWG to forecast precipitation from Z500 for several seasons (winter and summer) in several locations for  $T = 5$  and  $T = 10$  day lead times.

235 The difference of the forecast correlation skills between the four studied locations may be related to the variation of the local climate from one region to an other. The studied areas are in different climate types according to Köppen-Geiger’s climate

**Table 4.** Correlation between observations and the median of 100 simulations for both seasons winter (DJF) and summer (JJA) for a lead time of 5 days

<b>Location</b>	<b>Correlation DJF</b>	95% confidence interval	<b>Correlation JJA</b>	95% confidence interval
<b>Berlin</b>	0.50	0.48 – 0.56	0.22	0.21 - 0.23
<b>Madrid</b>	0.53	0.51 – 0.55 - 0.59	0.29	0.27 - 0.30
<b>Orly</b>	0.58	0.56 – 0.59	0.23	0.20 - 0.24
<b>Toulouse</b>	0.40	0.39 – 0.44	0.18	0.15 - 0.19

classification map (Peel et al., 2007). From the south western side of Europe, Madrid is in the arid zone (Peel et al., 2007), which indicates that convective rains are less significant, so that the origin of precipitation might be the result of humidity coming from the Atlantic. Conversely, Berlin is located in a cold zone characterised by warm summer and the absence of a dry season (Peel et al., 2007), so that the precipitation could be the result of both convective rains and Atlantic humidity.

In this paper, we decided (for simplicity) to use the same analogs to forecast precipitation for those four stations. A refinement of the analog regions would be necessary when focusing on Madrid vs. Berlin.

### 4.3 Forecast probability skill

The skill scores CRPSS and correlation are computed for the four studied stations Orly Berlin, Madrid and Toulouse, as showed in illustrations represented in (Figure 4) and for lead times from 5 to 20 days. We represent skill scores for January and July in order to evaluate the skill of the SWG to predict precipitation in both seasons (winter and summer).

The CRPSS for persistence and climatology references show positive values for lead times of up to 20 days (Figure 4). The values of CRPSS with persistence reference (represented by squares) decrease with lead times, showing high values over 5 days. The CRPSS for climatology (triangles) show lower values, although positive. The correlation skill is positive for both seasons but higher in winter (January) than in summer (July). For a lead time of 5 days, the correlation is equal to 0.59 for Madrid, 0.50 for Berlin and to 0.40 for Toulouse. For a lead time of 10 days, it is equal to 0.42 for Madrid, 0.30 for Berlin and to 0.41 for Toulouse.

The SWG was tested in previous work Yiou and Déandréis (2019) to forecast North Atlantic oscillation (NAO) and temperature in western Europe. Comparing the performance of the SWG to forecast those different meteorologic variables, we notice that the model shows good performance to forecast the temperature and NAO in the winter, also the best performance of the model is at a lead time of 5 days. We find that the skill scores (CRPSS and correlation) decrease with lead of times. The forecast skill of the SWG shows variability from one location to another. However, the model was able to forecast temperature until 40 days in Berlin, Orly and Toulouse with positive skill scores.

From a visual inspection of the CRPSS and correlations, we chose to focus on lead times of  $T = 5$  days, for which the correlation exceeds 0.5 in the winter. It is rather low in the summer, due to convective events leading to a high precipitation

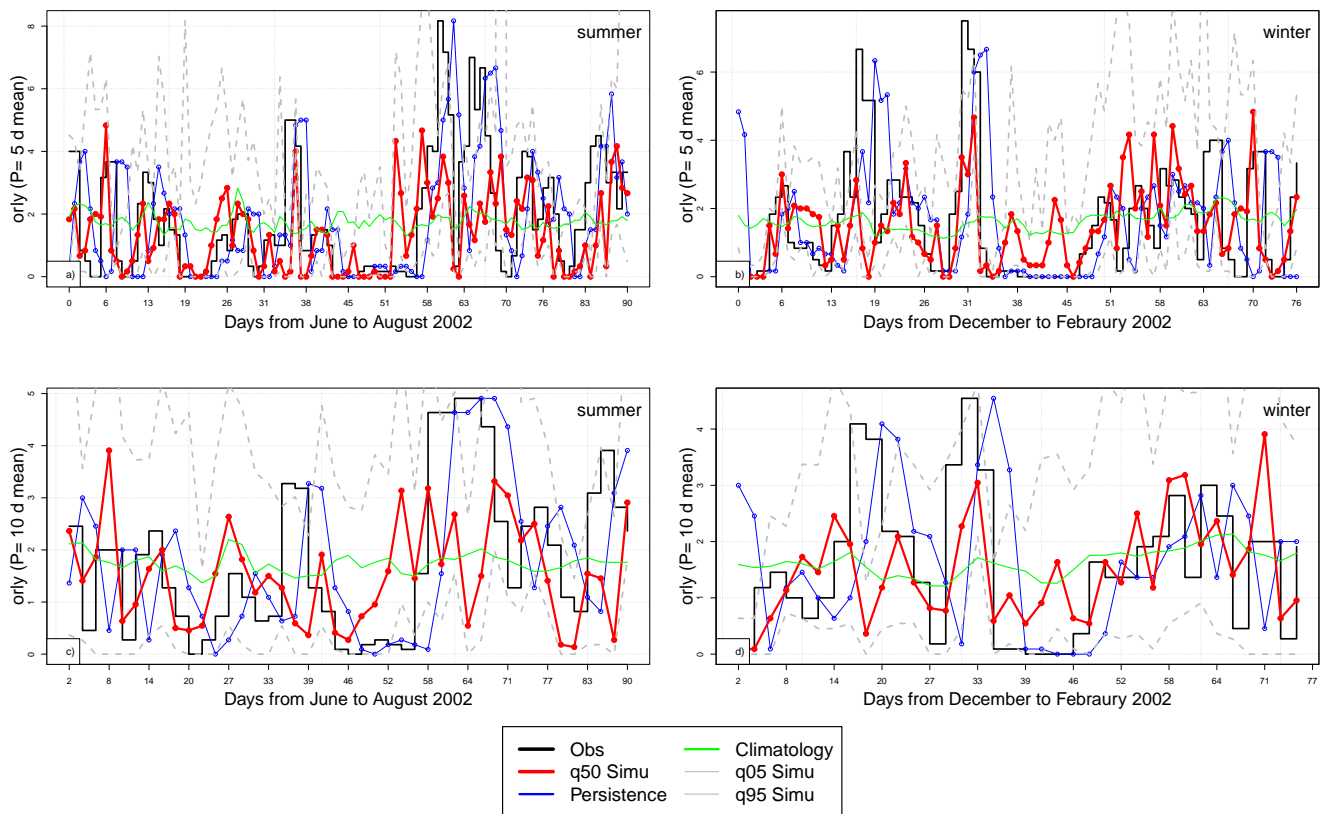


**Figure 3.** Time series of analog ensemble forecasts for 2002, for lead times of 5 days (top) and 10 days (bottom) for summer (June to August) a) and c) and winter (December to February) b) and d) for Orly. The median of 100 simulations is represented by red line. Black line represent observations values. Gray lines represent the 5th and 95th quantiles. Blue lines represent persistence forecasts and green lines represent the climatology forecasts. The y-axis represent the average of precipitation over  $T = 5, 10$

variability (from no rain to very high values). Correlation scores become barely significant for lead times of 20 days, so that, like temperature, the SWG should not be used beyond that horizon.

#### 4.4 Relation between weather regimes and CRPS

In this subsection, we investigate the role of North Atlantic weather patterns on the CRPS of the SWG precipitation simulations.

265 We start by comparing the frequencies of the weather regimes from the observations and the most frequent weather regime found in SWG simulations for a given lead time  $T = 5$  days. We find that the percentages are very similar (Figure 5). This means that the weather regimes of the simulated trajectories do not yield major biases for the summer or winter seasons.

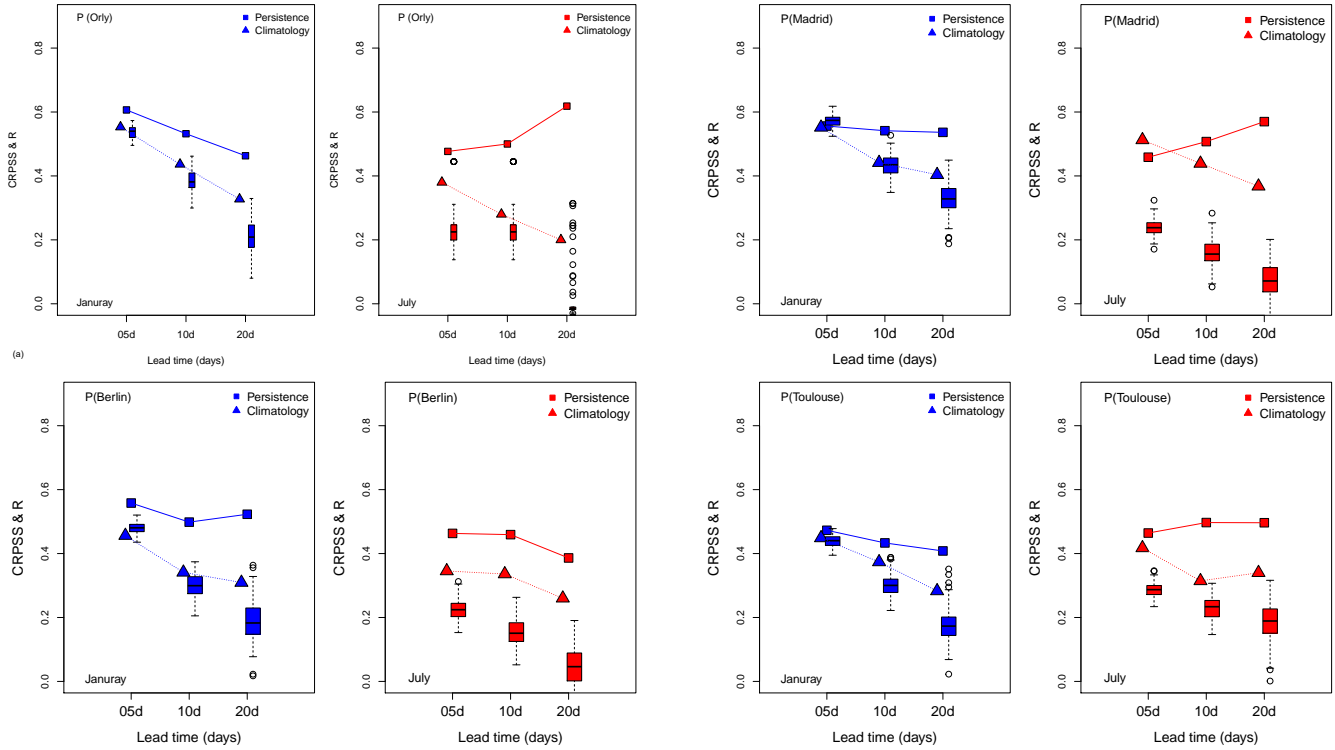


**Figure 4.** Skill scores for the precipitation of Orly, Madrid, Berlin and Toulouse for lead times of 5, 10, 20 days for January (blue) and July (red) for analogs computed from reanalyses of (a) NCEP and (b) ERA5. Squares indicate CRPSS where the Persistence is the baseline, triangles indicates CRPSS where the climatology is the reference, and box-plots indicates the probability distribution of correlation between observation and the median of 100 simulations for all days.

Then we look at the relation between weather regime and the CRPS, by using the most frequent weather regime and the two classes of quantiles of the CRPS that related to good quality of forecast (attributed to low values of  $CRPS \leq q_{25}$ ) and poor quality of forecast (attributed to high values of  $CRPS \geq q_{75}$ ). This relation is represented in Figure 6 for Orly and for the rest of the studied stations in Figure A1. We find a small, albeit significant, influence of specific weather regimes on the CRPS distribution for summer.

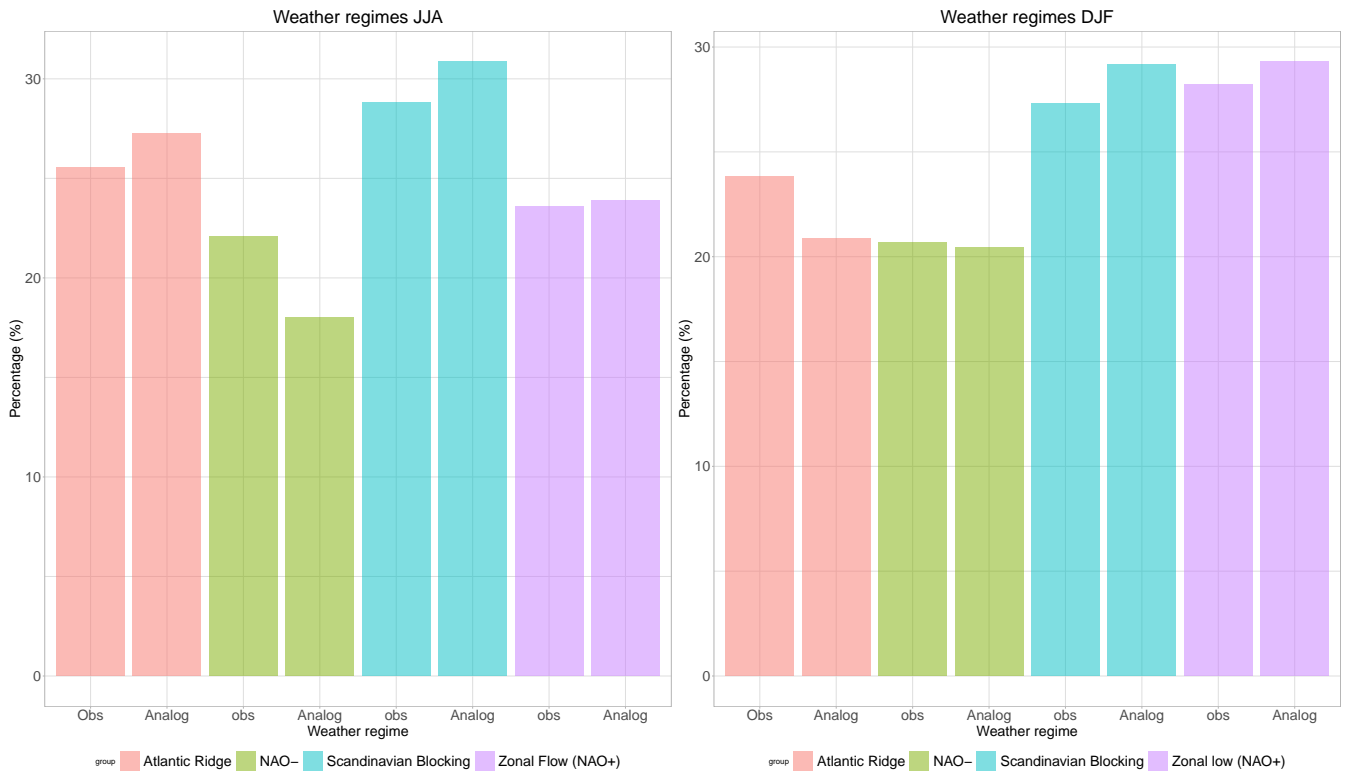


**Figure 5.** Percentage of each weather regime for observations dates (Obs) and the most frequent weather regime from SWG simulations between  $t_0$  and  $t_0 + T = 5$  days (Analog) over the period from 1948 to 2019 for summer (JJA) and winter (DJF). The percentage of weather regime are the same in Obs and Analog.

The weather regime signal for "good" forecasts depends on the season and the considered station. When the forecast has a low CRPS value (for Orly), we find that the Scandinavian Blocking regime slightly dominates (green bar in Figure 6a, b). This is also the case for Berlin (in winter) and Toulouse Figure A1 (b, j). The low CRPS values in Madrid are obtained for the Atlantic Ridge regime Figure A1 f.

The weather regime signal for "poor" forecasts also yields a dependence on the season and station. Higher CRPS values are obtained with the Atlantic Ridge regime in the summer for Orly (red line in Figure 6 c) and Berlin in winter and summer. The Atlantic ridge regime favors high CRPS values (i.e. poor forecasts) for Madrid in winter Figure A1 h. The Atlantic ridge regime favors high CRPS values for Toulouse in summer. The different impacts of the weather regimes on the studied areas is related to the position of the high and low pressure regions of each weather regime and their position regarding the studied areas.

This relation between predictability (or the CRPS distribution) and weather regimes, albeit weak, is consistent with previous work (Faranda et al., 2017). Similar relation were found between weather regimes over Europe and the Temperature in a recent

285 study by (Ardilouze et al., 2021) . We find that the sensitivity of the forecast to weather regime is larger for low values of CRPS and in the winter. The sensitivity of forecast skill to weather regimes is rather small on average, even for low lead times.

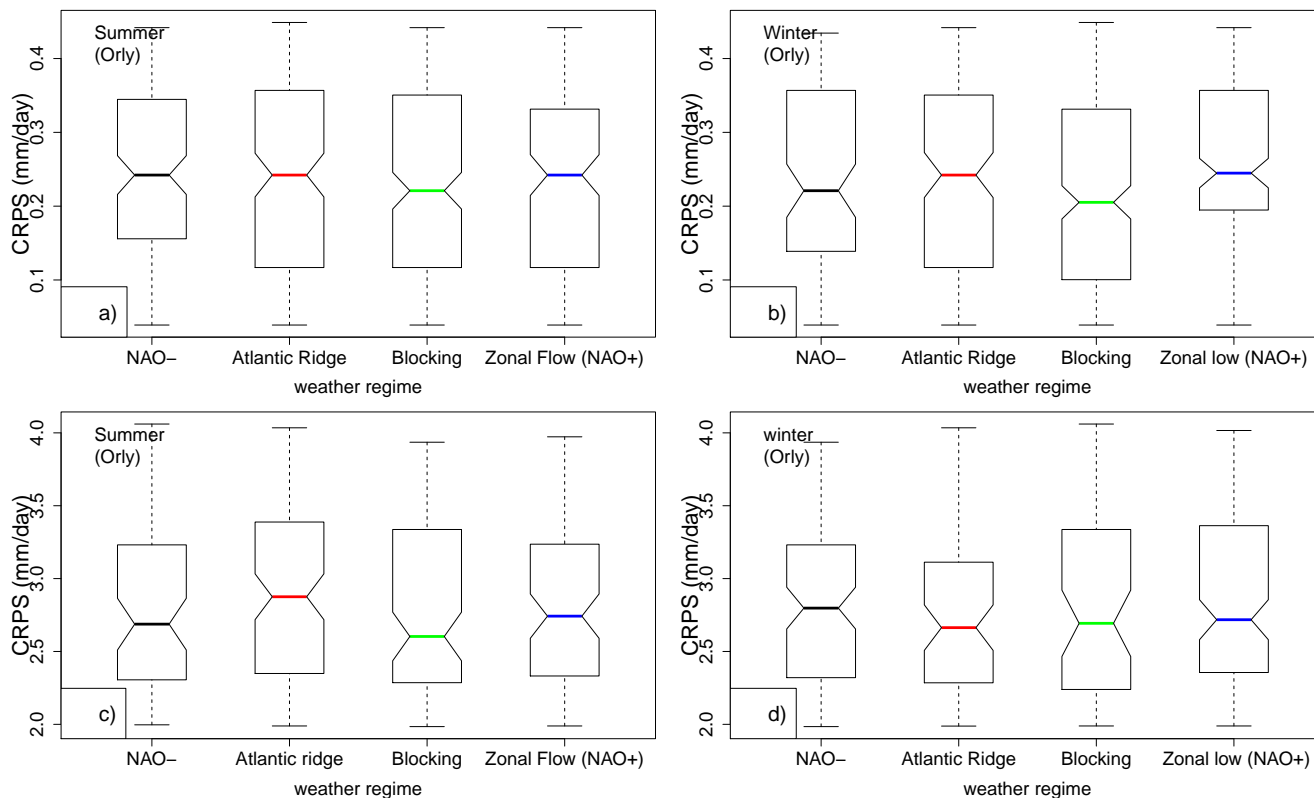


**Figure 6.** Relation between CRPS and weather regimes for Orly, for SWG forecasts with lead time  $T = 5$  days. Upper panels (a and b): CRPS value distribution conditioned on four weather regimes, when CRPS is lower than  $q_{25}$ . lower panels (c and d): CRPS is higher than  $q_{75}$ . The boxplots indicate the median ( $q_{50}$ ) of the distribution (thick bar). 25th ( $q_{25}$ ) and 75th ( $q_{75}$ ) quartiles (lower and upper segments). The upper whisker is:  $\min(1.5(q_{75} - q_{50}) + q_{50}, \max(CRPS))$  .

#### 4.5 Comparison with ECMWF forecast

We first compared the CRPSS of SWG forecasts for winter and summer with the CRPSS of ECMWF forecasts.

290 The CRPSS of ECMWF forecast is computed for different lead times going from 1 day to 10 day for the precipitation. It uses the climatology as a reference (Haiden et al., 2018). The values of CRPSS for Europe for 2020 decrease with lead times. They are about 0.16 in the summer (JJA) and 0.25 in the winter (DJF) for a lead time of  $T = 5$  days. The values of CRPSS for ECMWF for both seasons are computed over whole Europe (Haiden et al., 2018).

The CRPSS of SWG for a lead time of  $T = 5$  days showed in Table 2, and this suggests that the predictive skill of SWG is qualitatively promising for short lead times, compared with ECMWF forecasts.

295 A quantitative comparison was made by comparing the empirical cumulative distribution function (ECDF; (Hersbach, 2000)) of the CRPS of ECMWF and SWG forecasts for 5 days (Figure 7). We found that the values of CRPS of ECMWF forecast and SWG forecast are 80%, 39% 50% and 40 % equal or near to zero for respectively Orly, Berlin, Madrid and Toulouse, which indicates the small variations of the CRPS.

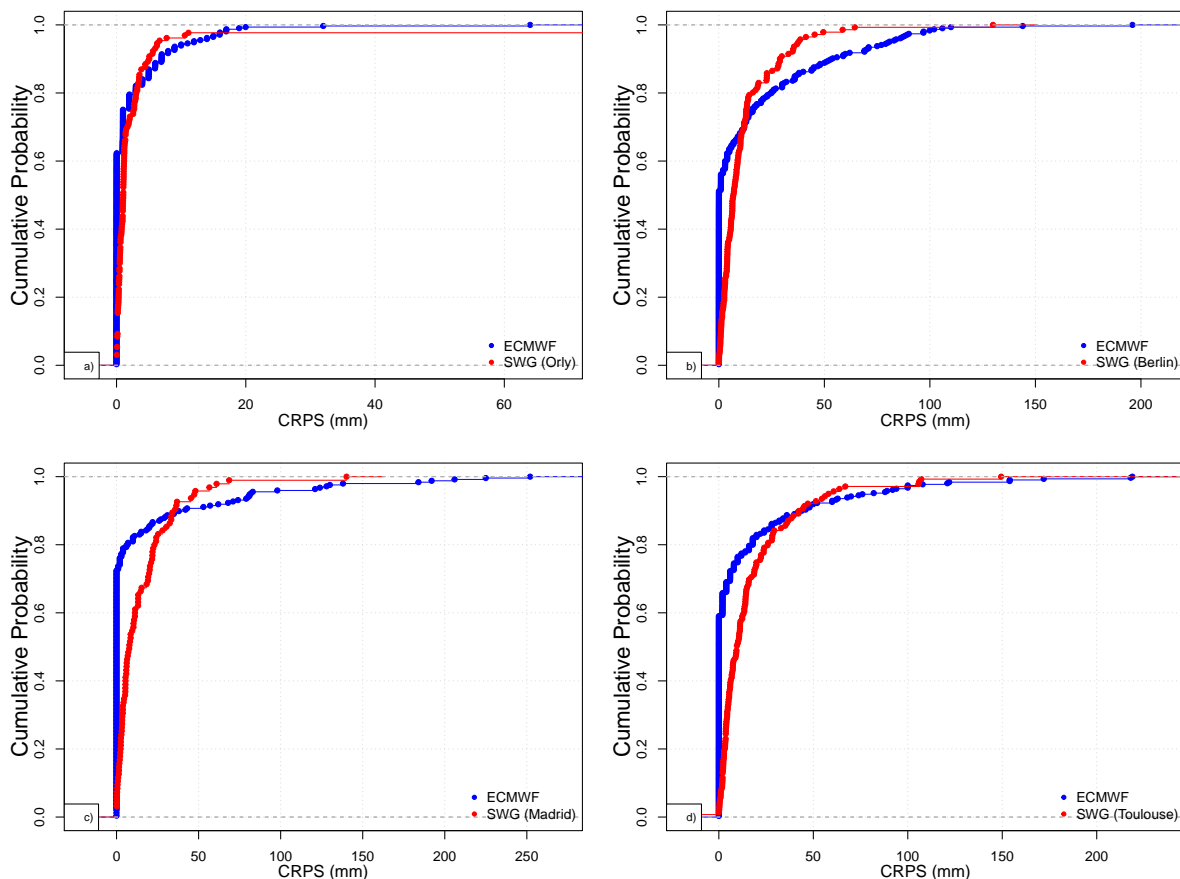


**Figure 7.** Empirical cumulative distribution function of the CRPS of ECMWF and SWG forecasts for 5 days for Orly (a), Berlin (b), Madrid (c) and Toulouse (d)

We used the Kolmogorov-Smirnov test (von Storch and Zwiers, 2001, Chap.1) to compare the probability distributions of the CRPS of SWG and ECMWF forecasts. The null hypothesis was that the two series of CRPS have the same distribution. This KS test allowed to reject this null hypothesis with  $p\text{-values} = 2.2 \cdot 10^{-16}$ . We conclude that the two series do not have the same distribution. A similar result was found by Ardilouze et al. (2021), where they compared the efficiency between ECMWF and CNRM forecasts. We also found that the maximum distance between both ECDFs is  $\approx 0.2$  (i.e.  $\approx 20\%$  of the whole range). One notable difference between SWG and ECMWF forecasts is that although the proportion of CRPS values close to zero is higher in ECMWF, the CRPS for the worse forecasts are much higher than those of SWG.



Finally, we computed the CRPSS for ECMWF forecasts taking as a reference the CRPS of SWG (Figure 8). We hence compute the CRPSS of ECMWF forecast by normalizing the CRPS by the CRPS of SWG forecast in Eq. 3.

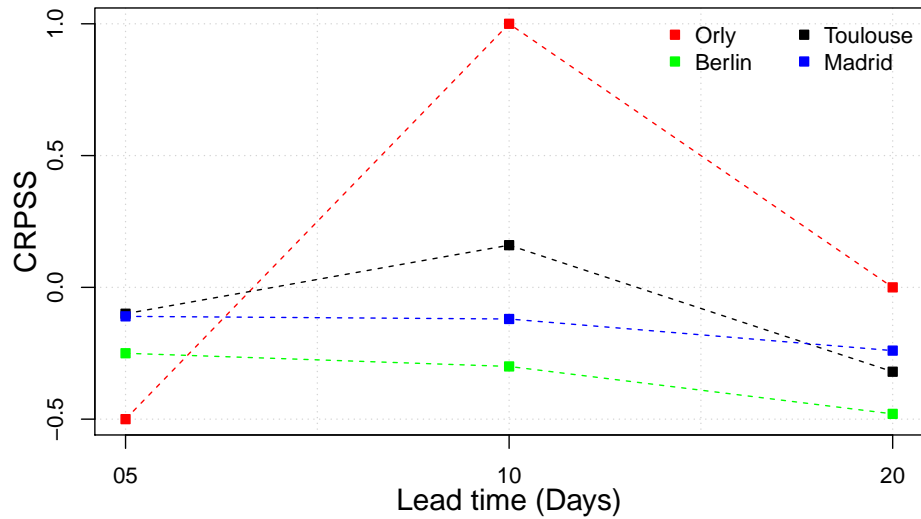


**Figure 8.** CRPSS of ECMWF forecasts using as a reference the CRPS of SWG, for lead times  $T = 5, 10$  and 20 days. It shows that for 5 days the SWG has a positive improvement comparing to the ECMWF forecast as the CRPSS are less than zero.

This evaluates the added value of the deterministic ECMWF forecast over the SWG forecast. We find that the ECMWF forecast has no improvement over the SWG forecast for a lead time of 5 days for the different studied areas because the CRPSS value are negative. For a lead time of  $T = 20$  days, the improvement of ECMWF forecast over the SWG is also negligible. There is a major improvement for a lead time of  $T = 10$  days for Orly and Toulouse. This confirms the relatively good skill of the SWG to forecast precipitation, compared to ECMWF.

## 5 Conclusions

In this work, we showed the performance of a stochastic weather generator (SWG) to simulate precipitation over different locations in western Europe and for various times scales from 5 to 20 days. The input of our model was analogs of geopotential heights at 500 hPa (Z500). The choice of such input was made in order to evaluate the impact of large scale circulation on local weather variables. SWG showed a good skill to predict precipitation for a lead time of 5 and 10 days from analogues of Z500.

This study complements the work of Yiou and Déandréis (2019), for precipitation. We explored the sensitivity of the SWG model on analogs computed from different geographical areas and from different reanalyses (ERA5 and NCEP). We found that the NCEP and ERA5 extended reanalyses provide better performances for simulations than ERA5 (1979–2019), due to its longer length ( $\approx 70$  years in NCEP vs.  $\approx 40$  years in ERA5). Therefore the length of the analog database does make a difference, as already suggested by Jézéquel et al. (2018a).

We evaluated the relation between the quality of the forecast and weather regimes over Europe, we found that low and high predictability was related to specific weather regimes, this dependence is more significant in winter than in summer, especially  
325 for the good predictability, it is found to be mainly related to Blocking.

A comparison with the ECMWF forecast system over Western Europe confirmed the good performance of the SWG quantitatively and qualitatively, for lead times  $T \leq 10$  days. Of course, the SWG model cannot replace a numerical weather prediction, as the SWG parameters (e.g. region of analogs) need to be tuned to local variables, and rely on the existence of a fairly large database to compute analogs. Here we used the same domain of circulation analogs for stations from Madrid to Berlin. Obviously, this region should be optimized for each individual station. Therefore, the main utility of the SWG forecast system is to  
330 make local ensemble simulations, where its performances can challenge a numerical weather prediction, if the parameters are well tuned.

This paper hence confirms the proof of concept to generate ensembles of (local) precipitation forecasts from analogs of circulation. Its performance relies on the relation between precipitation and the synoptic atmospheric circulation, which is  
335 verified for western Europe. Transposing this SWG to other regions of the globe requires observations covering several decades. Numerical weather models obviously do not yield this constraint.

*Code availability.* The code and data files are available at <http://doi.org/10.5281/zenodo.4524562>

*Author contributions.* MK performed the analyses. PY co-designed the analyses. CD and ST participated to the manuscript preparation.

*Competing interests.* The authors declare no competing interest.

340 *Acknowledgements.* This work is part of the EU International Training Network (ITN) Climate Advanced Forecasting of subseasonal Extremes (CAFE). The project receives funding from the European Union's Horizon 2020 research and innovation programme under the Marie Skłodowska-Curie Grant Agreement No 813844. We thank L. Magnusson for helpful discussions on the ECMWF data.

## **Appendix A: CRPS and weather regimes**

To avoid a tedious redundancy we deferred the figures of evaluation of the forecast quality by weather regimes to this appendix  
345 section.

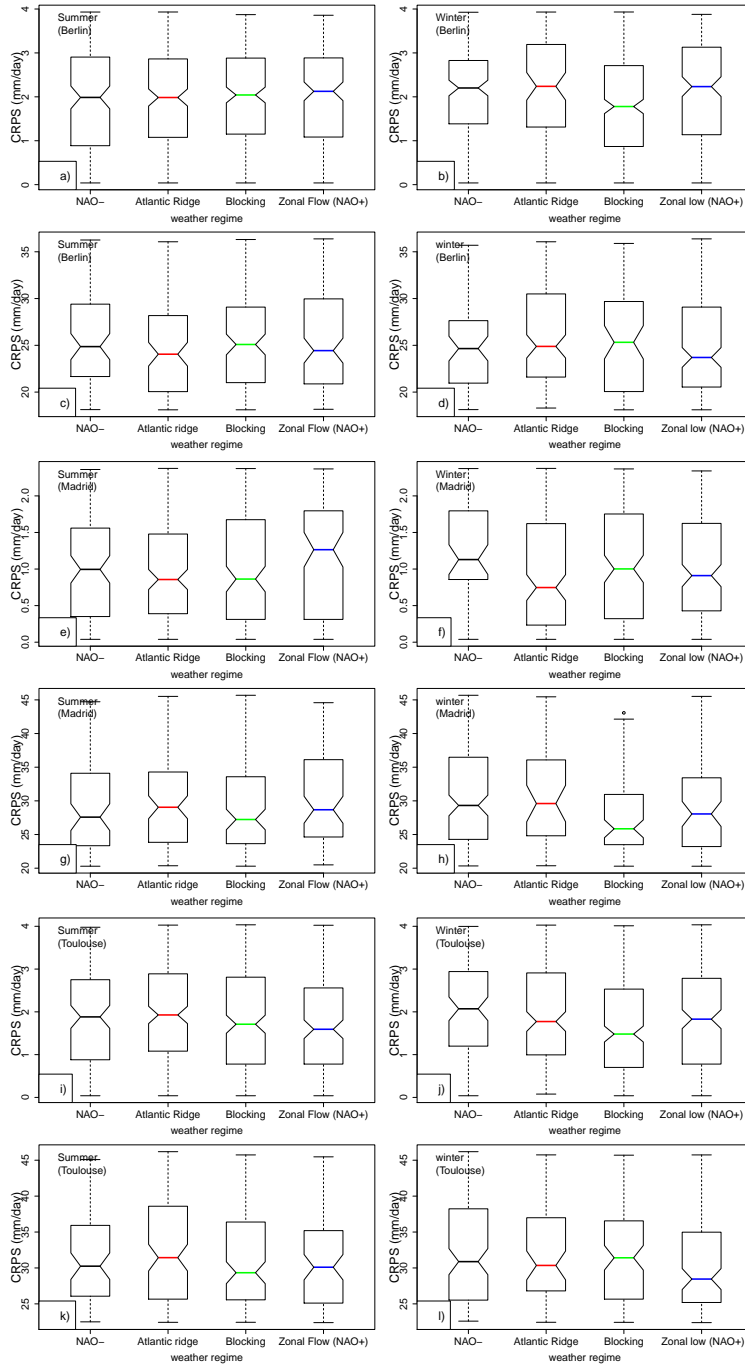


**Figure A1.** Relation between CRPS and weather regimes for Berlin (a–d), Madrid (e–h) and Toulouse (i–l), for SWG forecasts with lead time  $T = 5$  days. The panels (a, b, e, f, i and j) correspond to CRPS value distribution conditioned on four weather regimes, when CRPS is lower than  $q_{25}$ . The panels (c, d, g, h, k and l) correspond to higher CRPS value  $CRPS \geq q_{75}$ . The boxplots indicate the median ( $q_{50}$ ) of the distribution (thick bar).

## References

- Ailliot, P., Allard, D., Monbet, V., and Naveau, P.: Stochastic weather generators: an overview of weather type models, *Journal de la Société Française de Statistique*, 156, 101–113, 2015.
- Ardilouze, C., Specq, D., Batté, L., and Cassou, C.: Flow dependence of wintertime subseasonal prediction skill over Europe, preprint, *Atmospheric predictability*, <https://doi.org/10.5194/wcd-2021-32>, <https://wcd.copernicus.org/preprints/wcd-2021-32/>, 2021.
- Atencia, A. and Zawadzki, I.: A comparison of two techniques for generating nowcasting ensembles. Part I: Lagrangian ensemble technique, *Monthly Weather Review*, 142, 4036–4052, 2014.
- Blanchet, J., Stalla, S., and Creutin, J.-D.: Analogy of multiday sequences of atmospheric circulation favoring large rainfall accumulation over the French Alps, *Atmospheric Science Letters*, 19, e809, <https://doi.org/10.1002/asl.809>, <http://doi.wiley.com/10.1002/asl.809>, 2018.
- 355 Cassou, C., Minvielle, M., Terray, L., and Périgaud, C.: A statistical–dynamical scheme for reconstructing ocean forcing in the Atlantic. Part I: weather regimes as predictors for ocean surface variables, *Climate Dynamics*, 36, 19–39, <https://doi.org/10.1007/s00382-010-0781-7>, <http://link.springer.com/10.1007/s00382-010-0781-7>, 2011.
- Eckmann, J.-P. and Ruelle, D.: Ergodic theory of chaos and strange attractors, in: *The Theory of Chaotic Attractors*, pp. 273–312, Springer, 1985.
- 360 Faranda, D., Messori, G., and Yiou, P.: Dynamical proxies of North Atlantic predictability and extremes, *Scientific reports*, 7, 41 278, <https://www.nature.com/articles/srep41278.pdf>, 2017.
- Ferro, C. A. T.: A probability model for verifying deterministic forecasts of extreme events, *Weather and Forecasting*, 22, 1089–1100, <GotoISI>://000250413300011, 2007.
- Gabriel, K. R. and Neumann, J.: A Markov chain model for daily rainfall occurrence at Tel Aviv, *Quarterly Journal of the Royal Meteorological Society*, 88, 90–95, 1962.
- 365 Ghil, M., Chekroun, M., and Simonnet, E.: Climate dynamics and fluid mechanics: Natural variability and related uncertainties, *Physica D*, 237, 2111–2126, <https://doi.org/10.1016/j.physd.2008.03.036>, 2008.
- Haiden, T., Janousek, M., Bidlot, J., Buizza, R., Ferranti, L., Prates, F., and Vitart, F.: Evaluation of ECMWF forecasts, including the 2018 upgrade, *European Centre for Medium Range Weather Forecasts*, 2018.
- 370 Haylock, M. R., Hofstra, N., Tank, A. M. G. K., Klok, E. J., Jones, P. D., and New, M.: A European daily high-resolution gridded data set of surface temperature and precipitation for 1950–2006, *J. Geophys. Res. - Atmospheres*, 113, doi:10.1029/2008JD010 201, <GotoISI>://000260598000009, 2008.
- Hempelmann, N., Ehbrecht, C., Alvarez-Castro, C., Brockmann, P., Falk, W., Hoffmann, J., Kindermann, S., Koziol, B., Nangini, C., Radanovics, S., Vautard, R., and Yiou, P.: Web processing service for climate impact and extreme weather event analyses. *Flyingpigeon* (Version 1.0), *Computers & Geosciences*, 110, 65–72, <https://doi.org/10.1016/j.cageo.2017.10.004>, <https://github.com/bird-house/blackswan>, 2018.
- 375 Hersbach, H.: Decomposition of the Continuous Ranked Probability Score for Ensemble Prediction Systems, *WEATHER AND FORECASTING*, 15, 12, 2000.
- Hersbach, H., Bell, B., Berrisford, P., Hirahara, S., Horányi, A., Muñoz-Sabater, J., Nicolas, J., Peubey, C., Radu, R., and Schepers, D.: The ERA5 global reanalysis, *Quat. J. Roy. Met. Soc.*, 146, 1999–2049, 2020.
- 380 Jolliffe, I. T. and Stephenson, D. B.: *Forecast verification: a practitioner’s guide in atmospheric science*, John Wiley & Sons, 2011.

- Jézéquel, A., Yiou, P., and Radanovics, S.: Role of circulation in European heatwaves using flow analogues, *Climate Dynamics*, 50, 1145–1159, 2018a.
- Jézéquel, A., Yiou, P., Radanovics, S., and Vautard, R.: Analysis of the exceptionally warm December 2015 in France using flow analogues, *Bulletin of the American Meteorological Society*, 99, S76–S79, 2018b.
- 385 Kimoto, M.: *Studies of Climate Variability Using General Circulation Models*, in: *Earth Planets and Space*, 2001.
- Kistler, R., Kalnay, E., Collins, W., Saha, S., White, G., Woollen, J., Chelliah, M., Ebisuzaki, W., Kanamitsu, M., Kousky, V., van den Dool, H., Jenne, R., and Fiorino, M.: The NCEP-NCAR 50-year reanalysis: Monthly means CD-ROM and documentation, *Bulletin of the American Meteorological Society*, 82, 247–267, <GotoISI>://000166742900003, 2001.
- 390 Klein Tank, A. M. G., Wijngaard, J. B., Können, G. P., Böhm, R., Demarée, G., Gocheva, A., Mileta, M., Pashiardis, S., Hejkrlik, L., Kern-Hansen, C., Heino, R., Bessemoulin, P., Müller-Westermeier, G., Tzanakou, M., Szalai, S., Pálsdóttir, T., Fitzgerald, D., Rubin, S., Capaldo, M., Maugeri, M., Leitass, A., Bukantis, A., Aberfeld, R., van Engelen, A. F. V., Forland, E., Mielus, M., Coelho, F., Mares, C., Razuvaev, V., Nieplova, E., Cegnar, T., Antonio López, J., Dahlström, B., Moberg, A., Kirchhofer, W., Ceylan, A., Pachaliuk, O., Alexander, L. V., and Petrovic, P.: Daily dataset of 20th-century surface air temperature and precipitation series for the European Climate Assessment: EUROPEAN TEMPERATURE AND PRECIPITATION SERIES, *International Journal of Climatology*, 22, 1441–1453, <https://doi.org/10.1002/joc.773>, <http://doi.wiley.com/10.1002/joc.773>, 2002.
- 395 Lorenz, E. N.: Atmospheric Predictability as Revealed by Naturally Occurring Analogues, *J. Atmos. Sci.*, 26, 636–646, 1969.
- Mastrantonas, N., Herrera-Lormendez, P., Magnusson, L., Pappenberger, F., and Matschullat, J.: Extreme precipitation events in the Mediterranean: Spatiotemporal characteristics and connection to large-scale atmospheric flow patterns, *International Journal of Climatology*, 41, 2710–2728, <https://doi.org/10.1002/joc.6985>, <https://onlinelibrary.wiley.com/doi/10.1002/joc.6985>, 2021.
- 400 Michelangeli, P., Vautard, R., and Legras, B.: Weather regimes: Recurrence and quasi-stationarity, *J. Atmos. Sci.*, 52, 1237–1256, 1995.
- Palmer, T. N.: Predicting uncertainty in forecasts of weather and climate, *Reports on Progress in Physics*, 63, 71–116, <GotoISI>://000085479700001, 2000.
- Peel, M. C., Finlayson, B. L., and McMahon, T. A.: Updated world map of the Köppen-Geiger climate classification, *Hydrol. Earth Syst. Sci.*, p. 12, 2007.
- 405 Peixoto, J. P. and Oort, A. H.: *Physics of climate*, American Institute of Physics, New York, 1992.
- Platzer, P., Yiou, P., Naveau, P., Filipot, J.-F., Thiébaud, M., and Tandeo, P.: Probability Distributions for Analog-To-Target Distances, *Journal of the Atmospheric Sciences*, 78, 3317 – 3335, <https://doi.org/10.1175/JAS-D-20-0382.1>, <https://journals.ametsoc.org/view/journals/atsc/78/10/JAS-D-20-0382.1.xml>, 2021.
- 410 Richardson, C. W.: Stochastic simulation of daily precipitation, temperature, and solar radiation, *Water Resources Research*, 17, 182–190, <https://doi.org/10.1029/WR017i001p00182>, <http://doi.wiley.com/10.1029/WR017i001p00182>, 1981.
- Ruelle, D.: Ergodic theory of differentiable dynamical systems, *Publications Mathématiques de l’Institut des Hautes Études Scientifiques*, 50, 27–58, 1979.
- Scaife, A. A., Arribas, A., Blockley, E., Brookshaw, A., Clark, R. T., Dunstone, N., Eade, R., Fereday, D., Folland, C. K., and Gordon, M.: Skillful long-range prediction of European and North American winters, *Geophysical Research Letters*, 41, 2514–2519, 2014.
- 415 Sivillo, J. K., Ahlquist, J. E., and Toth, Z.: An ensemble forecasting primer, *Weather and Forecasting*, 12, 809–818, <GotoISI>://000071577700008, 1997.
- Todorovic, P. and Woolhiser, D. A.: A stochastic model of n-day precipitation, *Journal of Applied Meteorology*, 14, 17–24, 1975.
- Toth, Z.: Intercomparison of Circulation Similarity Measures, *Mon. Wea. Rev.*, 119, 55–64, <GotoISI>://A1991FA68200003, 1991.

- 420 Toth, Z. and Kalnay, E.: Ensemble forecasting at NCEP and the breeding method, *MONTHLY WEATHER REVIEW*, 125, 3297–3319, <GotoISI>://A1997YJ55500014, 1997.
- Türkes, M., Sümer, U., and Kiliç, G.: Persistence and periodicity in the precipitation series of Turkey and associations with 500 hPa geopotential heights, *Climate Research*, 21, 59–81, <https://doi.org/10.3354/cr021059>, <http://www.int-res.com/abstracts/cr/v21/n1/p59-81/>, 2002.
- van den Dool, H. M.: *Empirical Methods in Short-Term Climate Prediction*, Oxford University Press, Oxford, 2007.
- 425 van der Wiel, K., Bloomfield, H. C., Lee, R. W., Stoop, L. P., Blackport, R., Screen, J. A., and Selten, F. M.: The influence of weather regimes on European renewable energy production and demand, *Environmental Research Letters*, 14, 094010, <https://doi.org/10.1088/1748-9326/ab38d3>, <https://iopscience.iop.org/article/10.1088/1748-9326/ab38d3>, 2019.
- Vitart, F., Ardilouze, C., Bonet, A., Brookshaw, A., Chen, M., Codorean, C., Déqué, M., Ferranti, L., Fucile, E., Fuentes, M., Hendon, H., Hodgson, J., Kang, H.-S., Kumar, A., Lin, H., Liu, G., Liu, X., Malguzzi, P., Mallas, I., Manoussakis, M., Mastrangelo, D., MacLachlan, C., McLean, P., Minami, A., Mladek, R., Nakazawa, T., Najm, S., Nie, Y., Rixen, M., Robertson, A. W., Ruti, P., Sun, C., Takaya, Y., Tolstykh, M., Venuti, F., Waliser, D., Woolnough, S., Wu, T., Won, D.-J., Xiao, H., Zaripov, R., and Zhang, L.: The Subseasonal to Seasonal (S2S) Prediction Project Database, *Bulletin of the American Meteorological Society*, 98, 163–173, <https://doi.org/10.1175/BAMS-D-16-0017.1>, <https://journals.ametsoc.org/doi/10.1175/BAMS-D-16-0017.1>, 2017.
- 430 von Storch, H. and Zwiers, F. W.: *Statistical Analysis in Climate Research*, Cambridge University Press, Cambridge, 2001.
- 435 Xoplaki, E., Luterbacher, J., Burkard, R., Patrikas, I., and Maheras, P.: Connection between the large-scale 500 hPa geopotential height fields and precipitation over Greece during wintertime, *Climate Research*, 14, 129–146, <https://doi.org/10.3354/cr014129>, <http://www.int-res.com/abstracts/cr/v14/n2/p129-146/>, 2000.
- Yiou, P. and Déandréis, C.: Stochastic ensemble climate forecast with an analogue model, *Geoscientific Model Development*, 12, 723–734, <https://doi.org/10.5194/gmd-12-723-2019>, <https://www.geosci-model-dev.net/12/723/2019/>, 2019.
- 440 Yiou, P., Goubanova, K., Li, Z. X., and Nogaj, M.: Weather regime dependence of extreme value statistics for summer temperature and precipitation, *Nonlinear Processes in Geophysics*, 15, 365–378, 2008.
- Yiou, P., Salameh, T., Drobinski, P., Menut, L., Vautard, R., and Vrac, M.: Ensemble reconstruction of the atmospheric column from surface pressure using analogues, *Climate Dynamics*, 41, 1333–1344, <https://doi.org/10.1007/s00382-012-1626-3>, <http://link.springer.com/10.1007/s00382-012-1626-3>, 2013.
- 445 Zamo, M. and Naveau, P.: Estimation of the Continuous Ranked Probability Score with Limited Information and Applications to Ensemble Weather Forecasts, *Mathematical Geosciences*, 50, 209–234, 2018.